THE ASTROPHYSICAL JOURNAL, 395:317–325, 1992 August 20

A SEARCH FOR ANISOTROPY IN THE COSMIC MICROWAVE BACKGROUND ON INTERMEDIATE ANGULAR SCALES

D. C. ALSOP,[1,2,3,4] E. S. CHENG,[5] A. C. CLAPP,[1,2,3,6] D. A. COTTINGHAM,[1,2,3,7] M. L. FISCHER,[1,2,3,6] J. O. GUNDERSEN,[1,8] E. KREYSA,[9] A. E. LANGE,[1,2,3,6] P. M. LUBIN,[1,8] P. R. MEINHOLD,[1,8] P. L. RICHARDS,[1,2,3,6] AND G. F. SMOOT[1,3,10]

Received 1991 December 5; accepted 1992 February 25

ABSTRACT

The results of a search for anisotropy in the cosmic microwave background on angular scales near 1° are presented. Observations were simultaneously performed in bands centered at frequencies of 6, 9, and 12 cm^{-1} with a multifrequency bolometric receiver mounted on a balloon-borne telescope. The statistical sensitivity of the data is the highest reported to date at this angular scale, which is of critical importance for understanding the formation of structure in the universe. Signals in excess of random were observed in the data. The experiment, data analysis, and interpretation are described.

Subject headings: cosmic microwave background

1. INTRODUCTION

The cosmic microwave background (CMB) is one of the few directly observable remnants of the early universe. Observations of the CMB anisotropy test theories of the formation of structure in the matter distribution (e.g., Bond 1989). To date, only a dipole anisotropy, which could be caused by the Earth's motion relative to uniform Hubble expansion, has been reliably detected (Smoot, Gorenstein, & Muller 1977). Observations on angular scales from the quadrupole to arcseconds have produced only upper limits on the anisotropy. The lowest upper limits are now approaching the $\Delta T/T = 1 \times 10^{-5}$ level (Readhead et al. 1989; Meinhold & Lubin 1991; Meyer, Cheng, & Page 1991).

Measurements of anisotropies at this small level have become increasingly more problematic. Emission from foreground sources, both galactic and extragalactic, is comparable to anisotropies of this amplitude. Several measurements which may have been limited by foreground source confusion (Boughn et al. 1992; Meyer et al. 1991; Davies et al. 1987) or which required source subtraction (Readhead et al. 1989) have already been reported. Since the spectra of the foreground sources are different from that of a CMB anisotropy, spectral information can be used as a tool to constrain or subtract the contribution of foreground sources to any measured signal. The shape of the foreground spectrum suggests that the optimum wavelength for observation is in the millimeter-wavelength band. Emission from the atmosphere is relatively large at these wavelengths so careful choice of observation frequency and observing site is essential to preventing instability in the atmosphere from limiting the sensitivity of an observation.

Because it is difficult to design an observation that is sensitive to anisotropies over a broad range of angular scale, observations can be characterized by the scale for which they are optimized. Small-scale, $\theta < 2'$, searches are most sensitive to secondary anisotropies produced by reionization at moderate redshift. Large-scale, $\theta > 5°$, searches probe scales greater than the horizon size at recombination and thus provide information on the primeval perturbation spectrum. Intermediate-scale searches seek to measure the perturbations responsible for the structure in the galaxy distribution on 1 to 100 Mpc scales. General considerations based on the observed velocities of galaxies suggest that the amplitude of anisotropies on intermediate angular scales should be several $\times 10^{-5}$ (Juszkiewicz, Gorski, & Silk 1987).

We report below the results of an experiment to search for CMB anisotropies on 1° angular scales. The observation was performed simultaneously in three millimeter-wave bands from a balloon gondola flown at an altitude of 30 km to reduce atmospheric emission.

2. INSTRUMENT

The instrument was an off-axis, Gregorian telescope with a 1 m diameter primary mirror, a chopping secondary mirror and a ^{3}He-cooled, bolometric photometer as the receiver. The underfilled optics defined a 0.°5 FWHM beam. The beam position was sinusoidally modulated 1.°3 peak-to-peak (pp) in azimuth by the rotation of the secondary mirror at a frequency of 6.1 Hz. The telescope pointing was controlled to $\pm 1'$ by the combination of an azimuthal reaction wheel and an elevation drive. The pointed telescope was originally designed for observations at 90 GHz with a coherent receiver (Meinhold et al. 1992; Chingcuanco, Lubin, & Meinhold 1990). It was outfitted with a new secondary mirror, a new chopping mechanism, new baffles, an in-flight calibration mechanism, and additional electronics to make it suitable for the bolometric receiver (Fischer et al. 1992). The data described in this paper are from the second flight of this receiver.

[1] Center for Particle Astrophysics; University of California, Berkeley.
[2] Department of Physics, University of California, Berkeley.
[3] Space Sciences Laboratory, University of California, Berkeley.
[4] Current postal address: Department of Radiology, Hospital of the University of Pennsylvania, 3400 Spruce Street, Philadelphia, PA 19104.
[5] NASA/Goddard Space Flight Center, Bldg. 21-G54, Code 6850, Greenbelt, MD 20771.
[6] Current postal address: Department of Physics, University of California, Berkeley, CA 94720.
[7] Current postal address: Universities Space Research Association, NASA/GSFC, Code 685.3, Greenbelt, MD 20771.
[8] Department of Physics, University of California, Santa Barbara, Santa Barbara, CA 93106.
[9] Max-Planck-Institut für Radioastronomie, Auf dem Hugel 69, D-5300 Bonn 1, Germany.
[10] Lawrence Berkeley Laboratory, University of California, One Cyclotron Road, Berkeley, CA 94720.

The modulation of the beam in azimuth produced signals at the chopping frequency and higher harmonics. Phase-synchronous demodulation with a chopper-synchronous sine-wave reference was applied to the signals. The demodulated beam pattern can be approximated as the difference between two 0°.54 FWHM Gaussian beams separated by 1°.06. Because of the brightness and size of the Earth and the balloon, low out-of-beam response was required from the optical system. The off-axis design of the telescope provided very low sidelobe response, and reflective baffles reduced the acceptance of bright, large angle sources. Modulation of the sidelobe response with chopper position, "chopped sidelobes," was not measured directly but the sidelobe rejection performance of the system was measured before flight at 3 and 9 cm^{-1} with the secondary mirror at the center and the two extrema of its motion. No significant differences in sidelobe response were found for the three secondary positions, suggesting that the "chopped sidelobe" response is much smaller than the "unchopped" response. Measurements were performed by scanning the telescope elevation above a fixed source. The "unchopped" response was found to be less than −70 dB at angles greater than 20° from the beam. The size and geometry of the telescope prevented us from testing other orientations.

The beam was divided into three bands centered at 6, 9, and 12 cm^{-1} by the selective reflection and transmission of interference filters. The transmission spectra of the three bands, which were measured in the laboratory, are shown in Figure 1. A separate detector measured each channel so all three bands were observed simultaneously. The detectors were ^{3}He-cooled, composite bolometers (Alsop et al. 1991). An additional detector, hereafter referred to as "blank," was mounted on the photometer with all optical access blocked to provide a check on noise and electronics systematics.

The system was calibrated in-flight by moving a partially reflecting membrane into the prime focus of the telescope at nonnormal incidence (Fischer et al. 1992). Rays reflected from the membrane were absorbed in an ambient temperature, 220 K, blackbody target whose temperature was monitored during flight. The reflectivity of the membrane was measured in the laboratory. This calibration method gave acceptable values for the emission from Venus in the earlier flight. We believe the accuracy of the calibration to have been better than 20%.

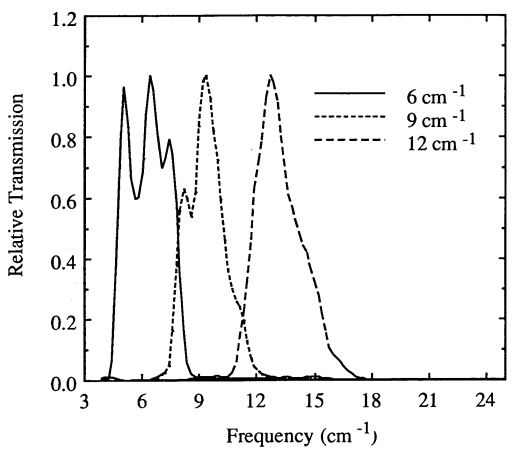

FIG. 1.—Measured transmission spectra of the three bands. 1 cm^{-1} equals 30 GHz.

3. OBSERVATION

The flight spanned approximately 10 hr from launch at 1:40 UT on 1990 July 2 from the National Scientific Balloon Facility in Palestine, Texas, until power was switched off at 11:20 UT in preparation for landing. The primary scientific observation was a search for CMB anisotropy which began at 8:36 UT and continued until 10:30 UT. Six calibrations were performed during the flight and Saturn was observed near the end of the flight to test the beam pattern and spectral response. A software error in the computer program of the guidance system prevented accurate pointing of the telescope from the beginning of the flight until the error was overcome just prior to the CMB scan.

Several hours before the CMB scan, a very high glitch rate in excess of the expected cosmic-ray events was observed in the raw signals of the 6 and 9 cm^{-1} bands. These events were correlated in the two bands and were not present in the 12 cm^{-1} and blank channels. The glitches were found to correlate with glitches in a semiconductor thermometer which monitored the temperature of the primary mirror. These two detectors and all the semiconductor thermometers were observed to be sensitive to RF when an auxiliary, 400 MHz, on-board transmitter was temporarily activated. The extreme sensitivity to the auxiliary transmitter was presumably due to some combination of its lower frequency (the main telemetry antennas operate at 1.4 GHz), different antenna pattern, and the different shielding and grounding of the transmitter. Based on these observations, the excess glitches were attributed to pulsed RF power incident on the receiver, possibly from radar. The insensitivity to RF of the detectors in the 12 cm^{-1} and blank channels was observed in the laboratory and may have been due to the different construction methods used for these higher background detectors. During the CMB search the glitch rate was low, though very small amplitude glitches attributable to RF were observed during some parts of the search. The phase-synchronous demodulation (PSD) of the detector signals also means that random glitches, like cosmic rays, contribute only to the noise of the observation because glitches occur both when the reference is positive and negative.

The CMB anisotropy scan was centered on γ UMi, a star at $\alpha = 15^h21^m$ and $\delta = 72°1'$. Two 37 minute observations were divided by a 13 minute calibration. Each 37 minute period contained seven complete scans. The scan pattern, which consisted of discrete azimuth steps, is displayed in the top of Figure 2. The seven integration points were separated by 1°.2 in azimuth, approximately 1° separation on the sky. Each fixed integration produced a single-difference measurement because of the demodulated beam pattern discussed above.

4. DATA REDUCTION

The detector data were telemetered to the ground as 16 bit, 4 ms samples of the amplified bolometer signals after antialiasing and AC-coupling filters. The data were first edited to remove telemetry failures, cosmic rays, and other glitches in the detector signals. Glitches were detected by removing the (lower frequency) optical signals and (higher frequency) microphonic noise with a digital bandpass filter and then identifying all events above a specified threshold as glitches. Data from 75 ms before until 200 ms after a glitch were removed. The remaining data were digitally lowpass filtered and phase-synchronously demodulated, using a sine-wave reference that was synchronous with the chopper. The PSD was performed twice for each

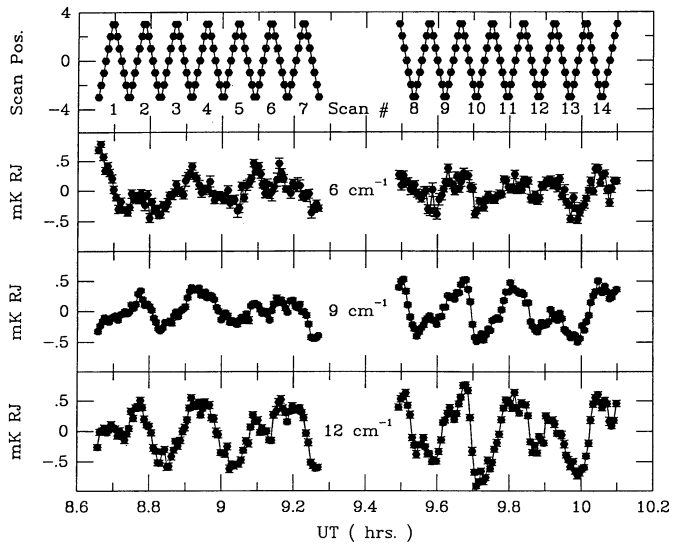

FIG. 2.—Scan position and phase-synchronous demodulated signals during the anisotropy search. Scan position is measured in degrees away from γ UMi parallel to the horizon. Signals are plotted in units of the signal produced by a 1 mK temperature difference between two Rayleigh-Jeans sources. An offset and a gradient over each half of the observation have been removed from the signals.

channel. The reference for the second PSD was shifted 90° in phase from that of the first. The first phase was chosen to be the phase at which a sky signal appears, as defined by the calibration signal; the other phase was therefore orthogonal to the sky phase and should have shown no sky signal. For the blank channel, the choices of phase were arbitrary so 0° and 90° relative to the chopper position were selected. The PSD produced a value for each cycle of the chopper motion, except when a glitch was detected.

The pointing data were acquired from a different telemetry system which sampled 3 times per second. The clocks of the two telemetry systems were synchronized on distinctive events in the detector signals which occurred during the calibrations. (The detector signals were present in both sets of telemetry data.) The azimuth data from the gyroscopes were used to determine the timing of the scan so that the observation could be divided into separate, stably pointed integrations. Data measured while the gondola was stably pointed within 0°.1 of the desired location were binned together. Data measured during the time the telescope was slewing between points were discarded. Roughly 100 complete chopper cycles occurred during each stably pointed integration so that many data points, s_i, were output by the PSD for each phase of each channel. An average signal for each integration, $S(I)$, was defined

$$S(I) = \sum_{i=1}^{N_{\rm chop}} \frac{s_i}{N_{\rm chop}},$$

for I between 1 and 196. An error estimate, Aerr (I), was also defined:

$$\text{Aerr } (I)^2 = \sum_{i=1}^{N_{\rm chop}} \frac{[s_i - S(I)]^2}{N_{\rm chop} - 1}.$$

The Aerr's calculated for the 9 cm^{-1} band and especially the 6 cm^{-1} band were found to be higher than expected during parts of the CMB scan. Further study discovered the presence of small-amplitude glitches which were correlated between the 6 and 9 cm^{-1} channels with relative amplitudes identical to the larger glitches observed earlier in the flight. The Aerr's were reduced when all s_i's with $|s_i - S(I)| > 3$ Aerr (I) were discarded and then the $S(I)$s and Aerr (I)s were recalculated. This procedure was repeated until no more s_i's were discarded. For white noise alone this additional deglitching method would remove about 0.3% of the data. For the real data, up to 20% of the s_i's during the worst integrations were removed from the 6 cm^{-1} data but typically less than 5% were removed due to the combined effect of the two deglitching methods. We believe that these small glitches were due to RF pulses incident on the receiver because of the glitches' similarity to the earlier, large glitches. The amplitudes of these glitches could have been a function of the chopper position and therefore could have caused a systematic signal after the PSD. The data were also analyzed without the second deglitching method in order to amplify any chopper correlated signals due to RF glitches, but only an increase in noise was observed. Systematic effects due to the binning and second deglitching procedures were studied with random simulated data sets of white noise alone and white noise plus $1/f$ (a model for the low-frequency noise discussed below). No significant departure from expected performance was found.

5. ANALYSIS

5.1. *Noise Characteristics*

The reduced data were examined for unexpected noise properties. Figure 2 shows the sky phase detector signals during the time of the observation after removal of a roughly −5 mK Rayleigh-Jeans (RJ) offset and a gradient. A pronounced low-frequency component, well in excess of detector noise, is apparent in the three sky phase channels. No such noise is present in the other phase of the detectors or in the blank channel so the noise was likely due to a millimeter-wavelength source. Since this low-frequency component was not correlated with scan position, it could not have been caused by a static, position-dependent signal like CMB anisotropy. There exists a significant correlation between the signals in the three channels but excess noise that was uncorrelated between the channels was also present (Fig. 3). The correlation allows the determination of a spectrum for the noise. The spectrum is inconsistent with two of the three important contributors to sky emission, oxygen and water, but is marginally consistent with the spectrum of ozone. If the correlated noise were due to ozone clouds, the uncorrelated noise must then be due to a different atmospheric component, a nonatmospheric source or substantially different near-field beams for the three bands. A rapid rotation of the gondola performed as a systematic test late in the flight showed signal modulations similar in amplitude and spectrum to the noise during the CMB anisotropy scan, but the modulation rate was much more rapid, suggesting that the azimuth rotation modulated the signal. Only the balloon, the Earth, and the atmosphere did not rotate with the telescope so atmospheric emission or sidelobe pickup of the Earth or balloon are the likely noise sources.

Because the excess noise is mostly at low frequency, its effect on the data is less severe than might be expected from the time series plots. Noise spectra of the reduced data for the sky phase signals show excess noise that drops very rapidly with increasing frequency. This suggested that the noise in the observation could be improved by highpass filtering the data in time.

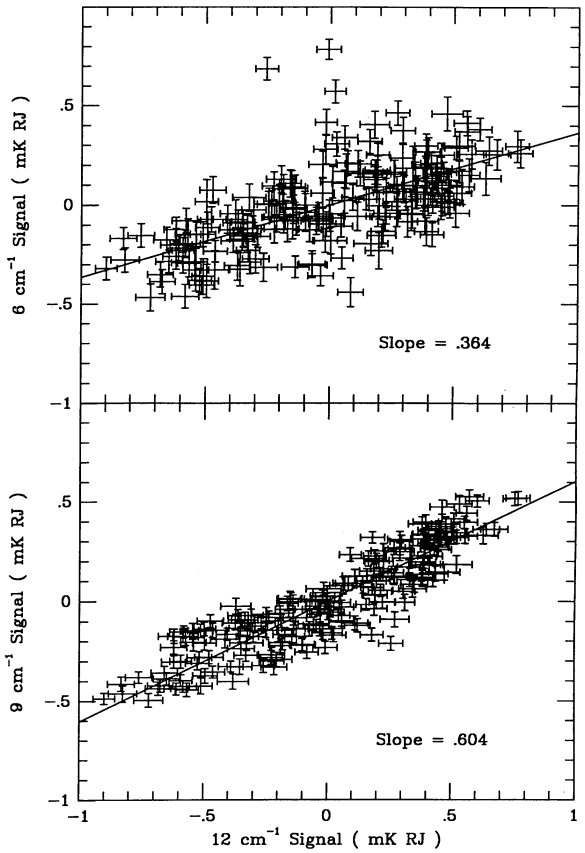

FIG. 3.—The correlation of the demodulated signals between the three bands. The best-fit slopes for the correlation imply that the spectrum of the noise is steeper than that of a Rayleigh-Jeans source. Uncorrelated noise in excess of the expected detector noise is also present on long time scales.

To evaluate the effect of highpass filtering on the noise, we compared the noise determined from the separate single integrations, Aerr (I), with the noise determined from the scatter of all the $S(I)$s, Berr. Any possible contribution from a scan-synchronous signal, such as CMB anisotropy or dust emission, was first removed from the data. A best-fit scan-synchronous signal at each of the seven scan positions was defined as the weighted average of the 28 fixed integrations at the position, i.e.,

$$\text{Sky}\ (n) = \sum_{j=1}^{14} W[I(n, j)]S[I(n, j)] + W[I(15 - n, j)]S[I(15 - n, j)]\ ,$$

where

$$W[I(n, j)] = \frac{\{\text{Aerr}\ [I(n, j)]\}^{-2}}{\sum_{k=0}^{13} [\{\text{Aerr}\ [I(n, k)]\}^{-2} + \{\text{Aerr}\ [I(15 - n, k)]\}^{-2}]}\ ,$$

and

$$I(n, j) = n + 14j \quad \text{for } j \leq 6;$$
$$= 8 - n + 14j \quad \text{for } j \geq 7\ .$$

Berr was then defined

$$\text{Berr}^2 = \sum_{j=0}^{13} \sum_{n=1}^{7} \left[\frac{\{S[I(n, j)] - \text{Sky}\ (n)\}^2}{\text{Aerr}\ [I(n, j)]^2} + \frac{\{S[I(15 - n, j)] - \text{Sky}\ (n)\}^2}{\text{Aerr}\ [I(15 - n, j)]^2} \right].$$

Berr better estimates the true noise in the observation because the Aerr (I)s are insensitive to noise with a period greater than a single integration duration, approximately 20 s, while the CMB observation is very sensitive to such noise. The Aerr (I)s could not be directly compared to Berr when a highpass filter is applied to the data because some of the noise power due to the Aerr (I)s would be filtered out by the highpass filter, even for white noise. We compared the two noise estimates by generating simulated data sets of uncorrelated Gaussian noise with rms noise equal to the Aerr (I)s and then determined the distribution of Berr calculated from these simulated data sets. The most likely value of Berr for the simulated data sets was defined as simulated Berr. The ratio, (actual Berr/simulated Berr), tests the uncorrelated, Gaussian noise assumption over the bandwidth defined by the highpass filter because it should be close to unity. Since the Aerr (I)s are consistent with detector noise, the above ratio is also a good test for excess noise.

The ratio was calculated for five highpass filters with cutoffs of 2.1, 5.1, 8.2, 11.4, and 14.4 mHz, respectively, and the results are displayed in Figure 4. The ratios for the orthogonal phase and the blank channel data average around 1.2. This suggests that the noise on the time scale of the chopper period was slightly smaller than the noise on the time scale of 20 s, the typical integration duration. The three sky phase ratios show very large deviations from unity when the frequency of the highpass cutoff is low because the previously discussed-low frequency component adds to the noise. As the frequency of the highpass cutoff is increased, the noise B ratio approaches a constant value of approximately 1.4. When a cutoff of 11.4 mHz is applied, all three sky phases reach this value and further highpass filtering does not affect the ratio. These results indicate that, with a cutoff of 11.4 mHz, near detector-noise can be achieved in all three sky phase channels. An 11.4 mHz highpass filter was applied to the data used in the following analysis unless otherwise stated.

5.2. *Determination of Signal*

Equipped with the above understanding of the noise, we averaged together all single integrations at the same scan position to produce seven data points per channel, Sky (n), as in the above equation. The error in Sky (n) was defined

$$\text{Serr}\ (n) = \frac{\text{Real Berr}}{\text{Sim. Berr}} \left[\sum_{j=0}^{13} (\{\text{Aerr}\ [I(n, j)]\}^{-2} + \{\text{Aerr}\ [I(15 - n, j)]\}^{-2}) \right]^{1/2}.$$

The factor of [real Berr/simulated Berr] was included to compensate for the tendency for the Aerr (I)s to underestimate the noise on long time scales. The resulting seven points with error bars were then tested for signal by use of standard χ^2 analysis. The highpass filtering removed 4 degrees of freedom from the seven points so only 3 degrees of freedom remain. The calculated χ^2 and probabilities are tabulated in Table 1. The 6 and 9

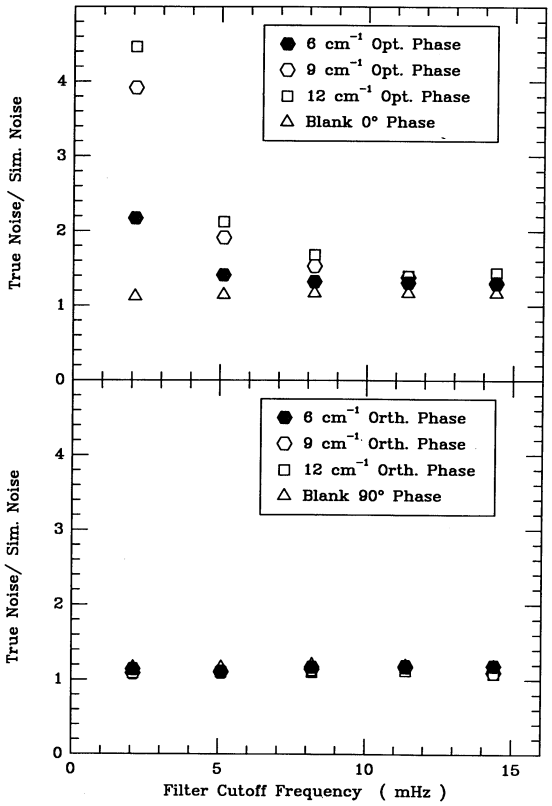

FIG. 4.—The ratio of the rms scatter in the demodulated detector signals to the scatter expected from the short-term error bars on each integration is plotted for signals that have been highpass filtered by a filter with the indicated cutoff frequency. The high values of the ratios in the three optical phase bands for low-frequency cutoffs indicate that significant excess noise is present on long time scales.

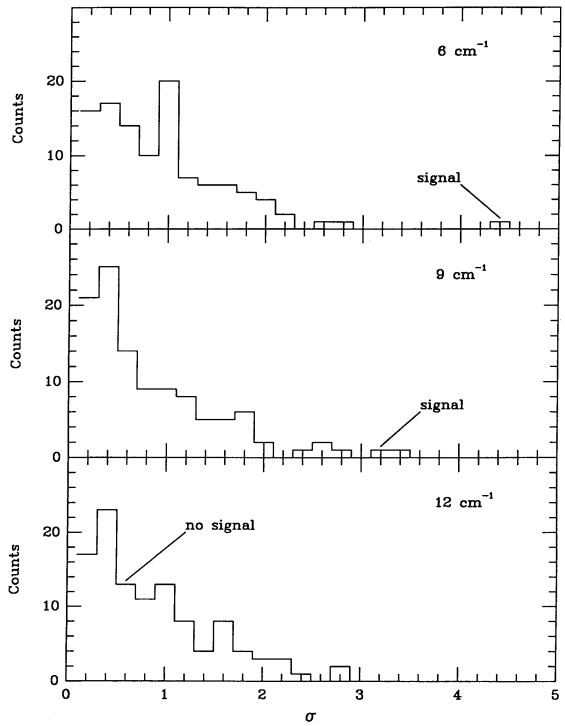

FIG. 5.—The integrated sky phase signals as a function of angle from γ UMi. High pass filtering has removed 4 degrees of freedom from the seven points for each channel. Signals in excess of the statistical noise are present in the 6 and 9 cm^{-1} channels.

cm^{-1} sky phase data are very improbable if due only to noise, and thus they represent a detection of some kind of scan-synchronous signal. The other data are all consistent with noise. Figure 5 shows the averaged data for the three sky phases. Most of the power in the detection was removed by the 14.4 mHz cutoff filter, indicating that the detection was dominantly at the one harmonic of the scan frequency removed by the 14.4 mHz cutoff filter but not the 11.4 mHz filter, 12.8 mHz.

Fourier transforms in time of the 196 single integration points, $S(I)$s, were calculated for each of the three sky phase channels. Because the observation was interrupted by a calibration and then resumed from a different starting position, the transform included a phase shift, $\Delta\phi(f) = \pi f/(3.2\ \text{mHz})$, when multiplying the second half of the observation in order to remain synchronous with the scan. An isolated peak was evident at 12.8 mHz in the 6 cm^{-1} band and could also be noticed at 9 cm^{-1}. There was no indication of excess noise in the neighborhood of 12.8 mHz in either channel. Histograms of the magnitude of all the Fourier components above 10 mHz are shown in Figure 6. They provide visual evidence of the significance of the detection.

A comparison of the two halves of the observation when analysed separately was also performed. In the absence of a constant systematic error, the two halves could be interpreted as two independent observations. The resulting sets of data

TABLE 1

PROBABILITIES OF BINNED DATA

Channel	χ^2	Reduced χ^2	Probability
6 cm^{-1}, sky phase	25.8	8.6	0.11×10^{-4}
9 cm^{-1}, sky phase	16.0	5.3	0.11×10^{-2}
12 cm^{-1}, sky phase	3.0	1.0	0.39
Blank, 0° from chopper	5.2	1.7	0.16
6 cm^{-1}, orthogonal phase	0.3	0.1	0.96
9 cm^{-1}, orthogonal phase	0.7	0.2	0.87
12 cm^{-1}, orthogonal phase	0.9	0.3	0.82
Blank, 90° from chopper	4.0	1.3	0.26

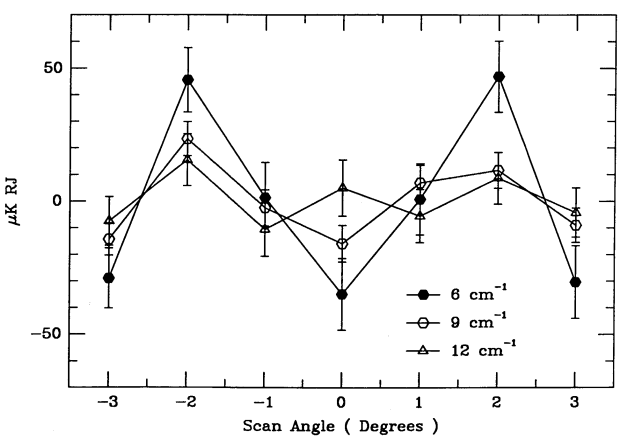

FIG. 6.—The distribution of noise when binned in frequency space. The time domain data were first Fourier-transformed and then the distribution of the signals in the frequency bins from 10 to 22.4 mHz was plotted. Scan-correlated signals could occur at only three frequencies, 12.8, 16.0, and 19.2 mHz. The boxes labeled "signal" represent the 12.8 mHz component.

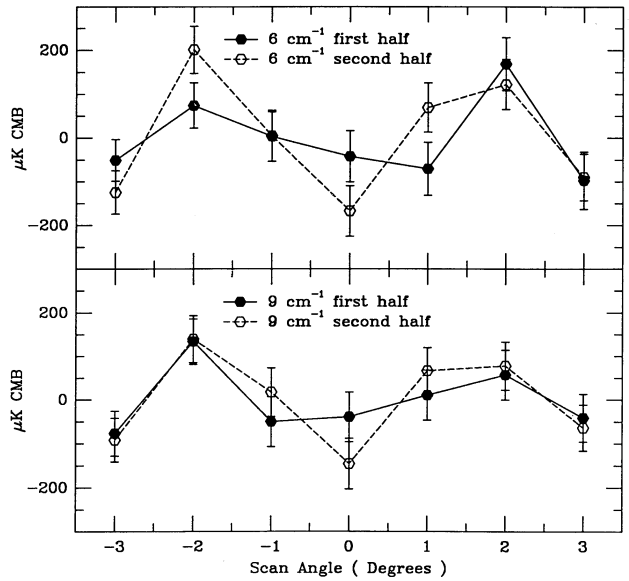

FIG. 7.—The results of dividing the observation into two halves and analyzing them separately for the 6 and 9 cm^{-1} channels. The integrated signals are plotted as in Fig. 5. The statistical consistency of the two halves is presented in Table 2.

were compared in Figure 7 for both the 6 and 9 cm^{-1} bands. Table 2 shows the probabilities of these results assuming the signal was the same for both halves and also the probabilities assuming zero signal. The results are consistent with a constant sky signal and provide an intuitively compelling argument for a scan-correlated signal.

6. DISCUSSION

A very significant scan-synchronous signal has been detected but detection of a scan-synchronous signal does not necessarily imply that CMB anisotropy has been detected. Below we consider a variety of systematic errors and galactic sources that could have mimicked a cosmic background anisotropy and estimate their contribution to the observed signal.

6.1. *Spectral Constraints*

The experiment was carefully designed to reduce sensitivity to a variety of systematic errors. The strength of the experiment is its multiband approach. If a spectrum of response can be assigned to a source of systematic error, then the possibility that it was present can be tested by comparing the expected spectrum with that observed. Figure 8 shows derived limits on the spectrum of the measured signal. The limits were calculated by assuming that the signals in the three sky phase channels varied identically with angle but with different amplitudes. The 6 cm^{-1} signal, which possesses only 3 degrees of freedom, was described by the parameters a, b, and c. In addition, two more parameters representing the relative amplitudes in the two other bands are necessary for the model: $S_{9/6}$ = 9 cm^{-1} signal/6 cm^{-1} signal and $S_{12/6}$ = 12 cm^{-1}/6 cm^{-1} signal. The total χ^2 was minimized with respect to all five parameters to yield maximum likelihood values. The model fits the data well, with a χ^2 of 2.9 for 4 degrees of freedom. The confidence contours are projections of the constant χ^2 surfaces onto the ($S_{9/6}$, $S_{12/6}$)-plane. The probabilities were estimated by adding random noise to the maximum likelihood signals and calculating new best values, thus determining the distribution of error. The plot in the ($S_{9/6}$, $S_{12/6}$)-plane can be viewed as a color-color diagram for the three bands. The values corresponding to several possible systematic errors and galactic sources are also plotted in Figure 8. They will each be discussed in more detail below. Spectra that are steeper than a Rayleigh-Jeans (R-J) spectrum are excluded with greater than 95% confidence.

TABLE 2

ANALYSIS OF DATA DIVIDED INTO HALVES

Channel	χ^2	Reduced χ^2	Probability
A. Probability of the Difference between Halves			
6 cm^{-1}	5.2	1.7	0.16
9 cm^{-1}	1.9	0.6	0.59
B. Probability of Halves			
6 cm^{-1}:			
First half	8.7	2.9	0.34×10^{-1}
Second half	21.7	7.2	0.75×10^{-4}
9 cm^{-1}:			
First half	6.2	2.1	0.10
Second half	11.5	3.8	0.93×10^{-2}

6.2. *Instrumental and Environmental Effects*

A variety of emission sources can be assigned spectra based on simple physical arguments. All significant atmospheric emitters at balloon altitudes have steeper than R-J spectra (their spectra are off-scale in Fig. 8). Emission from the Earth, the balloon, and the telescope mirrors and baffles should be R-J or steeper. These spectra are, however, relevant only if the beam illumination is identical for the three wavelength bands. Effects like diffraction can cause different illumination patterns on a source at different wavelengths. This is particularly important for sources far from the main beam, e.g., the Earth,

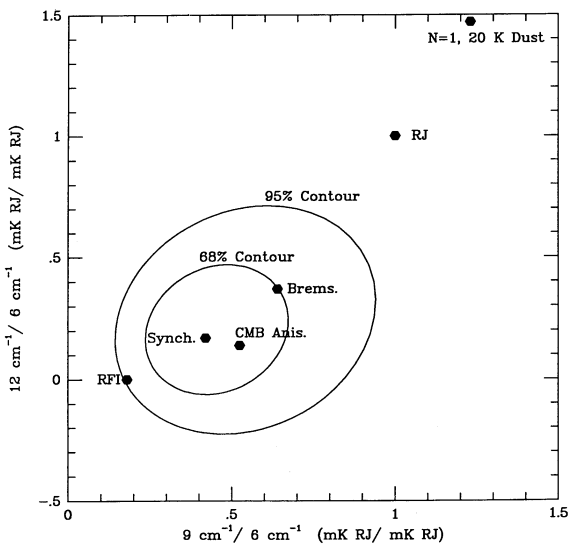

FIG. 8.—Spectral constraints on the observed scan-correlated signals. Contours constraining the ratios of the 9 and 12 cm^{-1} scan-correlated signals to the 6 cm^{-1} signal are plotted. Also shown are the ratios that would occur for a Rayleigh-Jeans source, synchrotron radiation from the galaxy, bremsstrahlung radiation from the galaxy, emission from interstellar dust at a temperature of 20 K with an emissivity proportional to frequency, and a CMB anisotropy. The point labeled RFI is an estimate of the relative response of the channels to interference from terrestrial radio frequency sources.

baffles, and the balloon. The sidelobe limits mentioned earlier were insufficient to eliminate the possibility of a contribution from 300 K sources far from the main beam: however, we believe that the single difference chop and the subtraction of an average offset from the final scan data would strongly reduce the effect of emission in the sidelobes. A source in the sidelobes capable of producing the observed signal must have features at 1° angular scale and must have remained in a fixed angular position relative to the telescope scan.

Several systematics have spectra which either were measured in flight or can be directly inferred from flight data. The low-frequency noise observed during the CMB scan showed a spectrum which was steeper than R-J, though there was not a perfect correlation between channels. A systematic change in efficiency or gain would produce a signal proportional to the offset signal. This offset is roughly R-J in spectrum so uniform gain change can be eliminated as a cause of the signal.

Much effort has been invested in the design of the chopping secondary since it is a potential source of noise and systematic error. The chopper has been designed for high stability in both amplitude and zero position since the offset signal must be a function of these two parameters at some level. In addition, the chopper has been equipped with high dynamic range position sensing and selectable zero position and amplitude set points. The amplitude and zero position were varied as a test during the flight to assess the effect of small changes. Using the results of these tests and the measured average zero and amplitude at each azimuth position during the CMB scan, we can eliminate the possibility of chopper instability causing the observed signal.

The above arguments all assume that the spectral response of the bands was well known. Calibration errors can lead to mistaken interpretation of the spectrum of flight signals. A scan of Saturn at the end of the flight provided a check on the relative response of the detector channels. Saturn is an approximately R-J source from 5 to 15 cm^{-1} (Roellig, Werner, & Becklin 1988). The spectrum inferred from the observation was consistent with R-J. Leaks in the filter bands at high frequency are a common problem for bolometric systems. The experiment was tested in the laboratory for leaks at wavelengths from 3 mm to below 10 μm. Leaks sufficient to explain the observed signal could be eliminated based on these tests. The response of the receiver to anisotropic emission from interstellar dust was also tested in flight when the gondola scanned rapidly across the galactic plane. A spectrum steeper than R-J was inferred as expected for standard dust models which confirms our understanding of the transmission of each band.

Non-radiative signal sources are also possible. An artificial signal must appear as a sine-wave signal at the 6.1 Hz frequency of the chopper motion. This could have occurred if the chopper driving circuits were connected to the detector amplifier circuits through some form of crosstalk. There are a variety of different phase shifts in such a model, i.e., the bolometer signal phase relative to the chopper motion, the phase shift of the crosstalk, and the phase between the chopper drive current and the chopper motion. It would be unlikely that a signal would appear only in the lock-in phase corresponding to a sky signal. A capacitively induced signal caused by mechanical coupling of the detector to the chopper motion faces similar arguments. These sources of offset would also have to have been varied synchronously with the scan. Since the offset from these sources was reduced to a value not measurable in 1 minute of integration on the ground, the fractional variation of the drive current or mechanical motion required to induce the observed signals would be greater than 10%. Such variations in the chopper motion are easily eliminated by reference to our chopper position data. Variation in the strength of the electrical or mechanical coupling between the chopper and the detectors is also possible but the gentle azimuth rotation of the gondola had minimal gravitational or mechanical effect on the solidly mounted receiver and electronics.

6.3. *Terrestrial Radio Transmissions*

The receiver was sensitive to RF power because bolometric detectors are sensitive to power input at any frequency. The coupling to the detectors was through the detector wires, not the optical system. Before flight it was observed that the detectors in the 6 and 9 cm^{-1} channels were much more sensitive to RF power at 1.4 GHz than the 12 cm^{-1} and blank channel detectors. This was presumably due to the different construction techniques used for the more sensitive detectors placed in the 6 and 9 cm^{-1} channels. In flight this "spectrum" of response was measured. RF was directly observed in flight in two forms: an offset change and sporadic glitches. The offset change was produced when the auxiliary transmitter previously mentioned was activated. This 400 MHz transmitter, for an as yet uncertain reason, had produced a much greater effect on the detectors than the telemetry antennas at 1.4 GHz both before and after launch. The offset change induced in flight was more than 100 mK R-J in the 6 cm^{-1} channel, near 20 mK R-J in the 9 cm^{-1} channel, and nonexistent in the 12 cm^{-1} and blank channels. A "spectrum" could thus be calculated. As described above, glitches which are believed to have been due to pulsed RF were observed in the 6 and 9 cm^{-1} channels. The glitches may have been caused by radar. The amplitude of the glitches were also used to derive a "spectrum" of RF response which was consistent with the other determination. The "spectrum" of RF response is plotted in Figure 8 and is just within the 95% contour. Since the "spectrum" may be a function of RF frequency and incidence angle, this should be used only as a rough guide to the relative RF response in the channels. Azimuth-modulated RF cannot be ruled out based on its "spectrum."

The requirements on an RF source capable of producing the detection are severe. The amplitude, position, or coupling to the detectors must have varied reproducibly with azimuth. If the source were the on-board telemetry antennas, some physical mechanism capable of recognizing azimuth position would be required. Two possible direction indicators were wind and gravity. Wind could have produced the observed signal by varying the position of the telemetry antennas or some RF absorbing or reflecting material on the gondola. Such a shear wind would have had to be stable to better than 2° in direction to produce the observed signal. Though these shear winds were not directly measured, the velocity of the gondola was a good measure of the stability of the total wind velocity at altitude. During the CMB scan, the direction of gondola motion varied by greater than 20°. Shear winds much more stable in direction than the total wind velocity seem unlikely. Gravity, in the absence of shear winds, is aligned with the axis of azimuth rotation so no change in gravity direction with azimuth could occur. Shear winds could tilt the gondola relative to the zenith so that a rotation would produce a small change in gravity direction. The gravity direction would then be slightly modulated by azimuth rotation. The 20° wind direction shift problem might not be as severe for this model since the tilt

direction of the gondola need not be the same as the wind direction. Tilt might be largely along the direction with the maximum surface area, for example.

RF sources external to the gondola are also possible. If the source were fixed to the Earth, angular stability requires a very distant source. The gondola traveled 80 km during the observation. To remain fixed in angle to less than 1°, a source must have been 4600 sin (α) km distant, where α is the angle between the source position and the balloon motion. The horizon at 30 km is 619 km distant. Since waves at radar frequencies do not reflect efficiently from the atmosphere, the source must have been within the horizon. This requirement translates to a requirement on the angular position of the source, $-8°$ (d/619 km) $< \alpha < 8°$ (d/619 km), where d is the distance from the balloon to the source. Angles 180° from these angles are also allowed. The response to the source must also have been unaltered by the elevation tracking which followed the observation region from 31° to 24° in elevation.

6.4. *Alternative Extraterrestrial Sources*

The possibility that the signal is astrophysical exists. Since standard dust models are steeper than R-J (Tielens & Allamondola 1987), they do not agree with the spectrum. Extrapolation of *IRAS* 100 μm data using a dust emissivity index of 1 and a temperature of 20 K produces an undetectable signal level in the 6 cm^{-1} channel. Synchrotron or bremsstrahlung emission are also possible sources. We simulated our observation on a 408 MHz map (Haslam et al. 1982) to constrain synchrotron and bremsstrahlung emission. Though the result does not display the same spatial features as the actual observation, the rms variation of less than 1 K R-J at 408 MHz can be used to constrain the spectral index of a source capable of producing the 30 μK R-J signal in the 6 cm^{-1} band. The emission in the 408 MHz map at high galactic latitude is believed to be dominated by synchrotron radiation. A typical spectral index of -2.7 yields an rms of 0.07 μK R-J at 6 cm^{-1}. An unknown fraction of the anisotropic emission in the 408 MHz map is due to bremsstrahlung emission. An upper limit on bremsstrahlung emission can be obtained by assuming that all of the anisotropy is due to bremsstrahlung. Its spectral index of -2.1 yields an rms of 2.8 μK R-J at 6 cm^{-1}, much less than the measured signal. Emission from a very cool component of the interstellar dust has been suggested (Wright 1982). Our spectral information can only constrain the temperature of such a dust to less than 11 K for positive emissivity indices. Anisotropic Compton distortion of the CMB caused by hot thermal electrons (Sunyaev & Zeldovich 1980) would produce signals of opposite sign in the 6 and 9 cm^{-1} bands so such a source is excluded by the constraints of Figure 8.

6.5. *Interpretation as CMB Anisotropy*

The data are consistent with a CMB anisotropy spectrum. To facilitate comparison with existing limits, constraints on the magnitude of anisotropy were derived assuming a Gaussian correlation function. They are displayed in Figure 9. The limits were calculated for a weighted sum of the 6 and 9 cm^{-1} channel data in order to obtain the highest signal-to-noise ratio. The χ^2-statistic used for analysis of the significance of the data in Table 1 was also used as the statistic for the limits in Figure 9 except the "noise" included a contribution from the CMB model being tested. The limit calculation accounts for the effects of data filtering and rotation of the sky during the observation. Also plotted is the most stringent upper limit published to date (Meinhold & Lubin 1991). Our data correspond to an amplitude of anisotropy which is consistent with their observation.

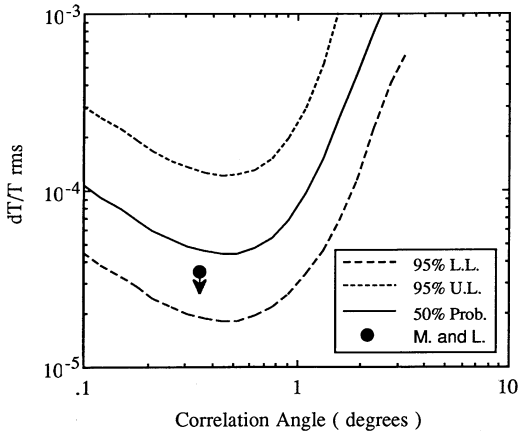

FIG. 9.—Derived limits on Gaussian-correlated CMB anisotropies. 95% upper and lower limits and the most probable value, 50%, are plotted vs. the correlation angle of the anisotropies. The filled circle represents the upper limit of Meinhold & Lubin (1991).

7. CONCLUSIONS

A multifrequency bolometric receiver has been used to perform a high sensitivity search for CMB anisotropy. Signals in excess of random were observed, but concerns about possible systematic errors prevent the interpretation of the signal as being uniquely cosmological in origin. The results illustrate the difficulty of positively identifying a CMB anisotropy when small instrumental effects and galactic emission may be present and underscore the need for systematic error rejection in the design of anisotropy searches. The existence of a null result, which is frequently used as an argument against the presence of systematics, cannot be used when signals are actually detected. The reliance on the null result as a success criteria may also lead to biases against the reporting of possible detections.

The presence of a large noise component at frequencies near the scan frequency and the sensitivity of the detectors in the 6 and 9 cm^{-1} channels to radio frequency signals reduced our confidence in this observation but the importance of these error sources can be dramatically reduced in future observations. The amplitude of the low-frequency noise was at least 5 times smaller in an earlier flight of the same experiment (Fischer et al. 1992). If the low-frequency noise was caused by the atmosphere, then higher altitude balloons, improved blocking of out-of-band leaks in the transmission spectra of the bands, and more rapid scanning will reduce the effect of the noise by orders of magnitude. Improvements in the baffle design and the quality of the primary mirror surface should make possible substantial reductions in any contributions to the noise from objects in the sidelobes of the telescope. Filters capable of reducing the radio-frequency sensitivity of the bolometric detectors by greater than 30 dB have already been developed. Radio-frequency detectors could also be used to veto the possibility of a significant contribution to any observed signal from terrestrial radio transmissions.

The observation reported here provides further evidence of the promise of balloon-borne bolometric receivers for observations of CMB anisotropy. In the absence of the low-frequency

noise and any scan correlated signal, this observation would have produced an upper limit on the rms $\Delta T/T$ of Gaussian anisotropies of less than 3×10^{-5}. Multichannel bolometric receivers make possible simultaneous observations at several frequencies through the same optics. Figure 8 illustrates the power of this observation strategy for restricting the range of possible systematic errors. Future flights incorporating the improvements detailed in the previous paragraph and more sensitive detectors are planned for the near future. These observations have the potential for measuring CMB anisotropies with $\Delta T/T$ as low as a few times 10^{-6}.

The authors would like to thank the staff of the National Scientific Balloon Facility in Palestine, Texas, for their hospitality and capable launch support. John Gibson, Casey Inman, and the Physics Department machine shops at Berkeley and Santa Barbara all contributed to the construction of the instrument. This work was supported by the Center for Particle Astrophysics through NSF cooperative agreement AST 8809616 and by the National Aeronautics and Space Administration through grants NSG-7205, FD-NAGW-2121, and NAGW-1062. One of us (D. C. A.) was partially supported by a NASA Graduate Student Researchers Program Fellowship.

REFERENCES

Alsop, D. C., Inman, C., Lange, A. E., & Wilbanks, T. 1992, Applied Optics, submitted
Bond, J. R. 1989, in Frontiers in Physics—From Colliders to Cosmology, ed. A. Astbury, B. A. Campbell, W. Israel, A. N. Kamal, & F. C. Khanna (Singapore: World Scientific), 182
Boughn, S. P., Cheng, E. S., Cottingham, D. A., & Fixsen, D. J. 1992, ApJ, 391, L49
Chingcuanco, A. O., Lubin, P. M., & Meinhold, P. R. 1990, J. Dynamic Sys. Meas. Contr., 112, 703
Davies, R. D., Lasenby, A. N., Watson, R. A., Daintree, E. J., Hopkins, J., Beckman, J., Sanchez-Almeida, J., & Rebolo, R. 1987, Nature, 326, 462
Fischer, M., et al. 1992, ApJ, 388, 242
Haslam, C. G. T., Salter, C. J., Stoffel, H., & Wilson, W. E. 1982, A&AS, 47, 1
Juszkiewicz, R., Gorski, K., & Silk, J. 1987, ApJ, 323, L1
Meinhold, P., et al. 1992, ApJ, submitted
Meinhold, P., & Lubin, P. 1991, ApJ, 370, L11
Meyer, S. S., Cheng, E. S., & Page, L. A. 1991, in After the First Three Minutes, ed. S. Holt, C. L. Bennett, & V. Trimble (New York: AIP), 113
Readhead, A. C. S., Lawrence, L. R., Myers, S. T., Sargent, W. L., Hardebeck, H. E., & Moffet, A. T. 1989, ApJ, 346, 566
Roellig, T. L., Werner, M. W., & Becklin, E. E. 1988, Icarus, 73, 574
Smoot, G. F., Gorenstein, M. V., & Muller, R. A. 1977, Phys. Rev. Lett., 39, 898
Sunyaev, R. A., & Zeldovich, Y. B. 1980, ARA&A, 18, 537
Tielens, A. G. G. M., & Allamandola, L. J. 1987, in Interstellar Processes, ed. D. J. Hollenbach & H. A. Thronson (Dordrecht: Reidel), 397
Wright, E. L. 1982, ApJ, 255, 401